Wide Frequency Range Active Damping of LCL-Filtered Grid Connected Converters

Abdelhady Ghanem*†, Mohamed Rashed†, Mark Sumner†, M. A. El-sayes* and I. I. I. Mansy*

* *Electrical Engineering Department, Mansoura University, Mansoura, Egypt.*
† *Department of Electrical and Electronics Engineering, University of Nottingham, Nottingham, UK.*
E-mail: aghanem_m@mans.edu.eg

Keywords: Parallel converters, Weak grid, Multi-resonance, Active damping.

Abstract

It can be challenging to guarantee the stability of grids with many converters with LCL filters connected due to the presence of multiple resonances within the system. This paper presents an active damping technique to mitigate multiple resonance effects and harmonics in power converters connected to weak grids. The proposed technique employs grid current and capacitor voltage feedback to achieve active damping for a wide range of multiple resonance frequencies. The effectiveness of the proposed wide frequency active damping and improved controller stability are demonstrated through frequency domain analysis and experimental results for single and parallel grid connected converters.

I. Introduction

Grid-connected voltage source power converters are widely used as interfaces and power conditioners for renewable energy generation [1]. Usually, *L*-filter or *LCL*-filter are adopted for decoupling between the power converter and grid as well as to attenuate the current harmonics at the switching frequency to meet grid codes and standards [1, 2]. Using *LCL*-filter allows lower inductance values, weight and cost for the same harmonic attenuation at the switching frequency compared to an *L*-filter. However, the *LCL*-filter introduces a resonance peak created by the interaction of the *LCL* filter and the grid impedance, which has to be damped in order to ensure system stability [3]. In addition, multiple resonance peaks can be introduced by the interactions between the output filters of paralleled grid connected converters which in turn challenges the stability of the current control loops of these converters [4]. Damping of these resonance peaks can be achieved using Passive or Active Damping (AD) approaches. Passive approaches rely on adding a real damping resistor but tend to be avoided due to additional losses [5]. In order to reduce the damping losses due to the damping resistance, additional passive elements (inductors or/and capacitors) have been added to the capacitor branch [6, 7]. However, the performance of these techniques is sensitive to grid impedance variations. Furthermore, additional passive elements are not desirable due to the increase in filter size and cost. AD approaches are preferred since they add virtual resistors to the system. Filter-based AD methods use a digital higher order filter in cascade with the current controller in order to filter out the resonance peak around the resonance frequency. First order and second order low pass filters [8], notch filters [9] and lead-lag compensators [10] have been applied to achieve this result. Therefore, no additional sensors are required and hence it is a sensor-less technique. The main disadvantage of this method is than an accurate system model is required and therefore it is sensitive to system parameter variations. Moreover, it significantly reduces the controller bandwidth. Filter capacitor current feedback is widely employed for AD [3, 11], however, additional current sensors increase the cost and reduce reliability. AD based on existing grid current feedback is presented in [12]. However, the AD is tuned to address a specific resonance frequency and cannot deal with variations of the resonance frequency without retuning the damping loop. Capacitor voltage can be used for AD as well. However, a derivative term is usually required in the damping path which causes noise amplification [13]. Capacitor voltage feedback through a High Pass Filter (HPF) has been also presented in [14]. However, it will de-stabilize the system if the system parameters vary over a wide range.

This paper proposes an AD approach based on the measured grid current and capacitor voltage feedback. This proposed method helps to stabilize the system and to improve the passivity of the converter output admittance to damp the resonances over a wide range of resonance frequencies caused by parallel connection of *LCL*-filtered grid connected power converters.

This paper is organized as follows: in section II, the system is described and the modelling of single and parallel grid connected converters are presented. Section III presents the participatory design procedures of the current control loop and proposed AD method. A frequency domain analysis and the investigation of the proposed AD technique with multiple parallel converters are presented in section IV. Experimental results verifying the proposed AD method for single and multiple grid connected converters are provided in section V. Finally, conclusions are drawn.

II. System description and modelling

In this section, description and modelling of a single grid connected converter as well as N-parallel grid connected converters are presented.

Single grid connected converter modelling

Fig. 1(a) depicts the diagram of a single grid connected converter with an *LCL*-filter. Grid current is controlled and the capacitor voltage is measured for grid synchronization. In order to obtain the overall system model, the grid connected converter shown in Fig. 1(a) is treated as two parts. The first part is the Norton equivalent model of the power converter including its control along with the *LCL*-filter. The second is the grid model as illustrated in Fig. 1(b).

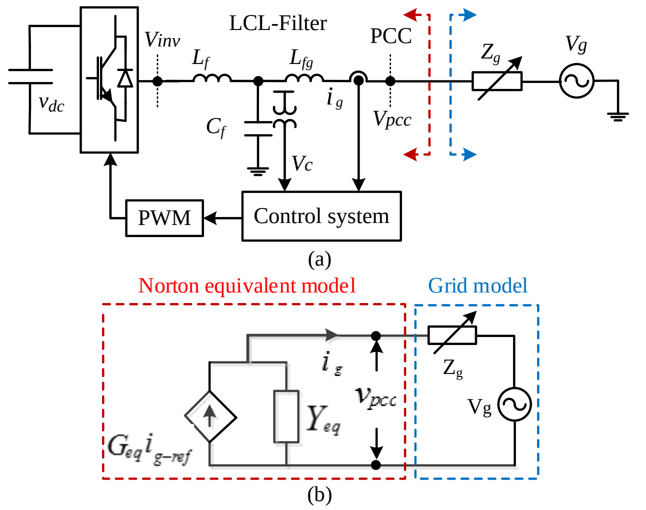

Fig. 1: (a): Grid connected converter. (b): Equivalent model.

The structure of a grid connected converter with the proposed AD system is shown in Fig. 2. The grid current and capacitor voltage are fed back through different HPFs. It is proposed to allow the capacitor voltage feedback loop to cope with low frequency resonant peaks while grid current damping loop is used to damp high frequency resonance peaks. As a result, wideband resonance frequency damping can be achieved.

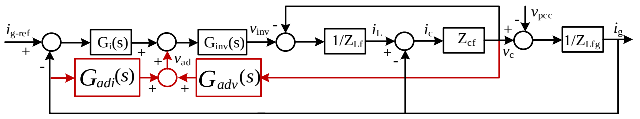

Fig. 2: Grid connected converter control with AD.

The parameters of each HPF are selected based on a participatory design method. The additional reference voltage v_{ad} from the AD loops is given by:

$$v_{ad} = v_c \frac{k_{adv} s}{s+\omega_{adv}} + i_g \frac{k_{adi} s}{s+\omega_{adi}} = v_c G_{adv}(s) + i_g G_{adi}(s) \quad (1)$$

From the block diagram shown in Fig. 2, the overall closed loop behavior of the single grid connected converter including the proposed AD is:

$$i_g = G_{eq} i_{\text{g-ref}} - Y_{eq} v_{pcc} \quad (2)$$

where;

$$G_{eq} = \frac{G_i(s) G_{inv}(s) G_{v_{inv}}^{i_g}(s)}{1 + G_i(s) G_{inv}(s)\, G_{v_{inv}}^{i_g}(s) - G_{adi}(s) G_{inv}(s)\, G_{v_{inv}}^{i_g}(s) - G_{adv}(s) G_{inv}(s)\, G_{v_{inv}}^{v_c}(s)}$$

$$Y_{eq} = \frac{-G_{adv}(s) G_{inv}(s) G_{v_{inv}}^{i_g}(s)\, G_{v_{pcc}}^{v_c}(s) - G_{v_{pcc}}^{i_g}(s) + G_{adv}(s) G_{inv}(s) G_{v_{pcc}}^{i_g}(s)\, G_{v_{inv}}^{v_c}(s)}{1 + G_i(s) G_{inv}(s)\, G_{v_{inv}}^{i_g}(s) - G_{adi}(s) G_{inv}(s)\, G_{v_{inv}}^{i_g}(s) - G_{adv}(s) G_{inv}(s)\, G_{v_{inv}}^{v_c}(s)}$$

$$G_i(s) = k_p + k_r . \frac{2\xi\omega s}{s^2 + 2\xi\omega s + \omega_n^2}, \qquad G_{inv}(s) = e^{-1.5 T_s s}$$

$$G_{v_{inv}}^{i_g} = \frac{1}{L_f L_{fg} C_f s (s^2 + \omega_{res}^2)}, \qquad G_{v_{inv}}^{v_c} = \frac{1}{L_{fg} C_f (s^2 + \omega_{res}^2)},$$

$$G_{v_{pcc}}^{i_g} = -\frac{L_f C_f s^2 + 1}{L_f L_{fg} C_f s (s^2 + \omega_{res}^2)}, \qquad G_{v_{pcc}}^{v_c} = \frac{1}{L_{fg} C_f (s^2 + \omega_{res}^2)},$$

$$\omega_{res} = \sqrt{\frac{L_f + L_{fg}}{L_f L_{fg} C_f}}$$

In order to obtain the overall closed loop response including the effect of grid impedance Z_g, v_{pcc} in (2) can be replaced by its equivalent shown in (3) which is obtained by applying Kirchhoff's current law at PCC in the circuit illustrated in Fig. 1(b).

$$v_{pcc} = \frac{Z_g G_{eq} i_{\text{g-ref}} + v_g}{1 + Y_{eq} Z_g} \quad (3)$$

From (2) and (3), the overall closed loop response including the effect of grid impedance is obtained as:

$$i_g = G_{cl} i_{\text{g-ref}} - Y_{cl} v_g \quad (4)$$

and the open loop transfer function can be obtained as:

$$G_{ol} = \frac{G_{eq}}{1 + Y_{eq} Z_g - G_{eq}} \quad (5)$$

where;

$$G_{cl} = \frac{G_{eq}}{1 + Y_{eq} Z_g}, \qquad Y_{cl} = \frac{Y_{eq}}{1 + Y_{eq} Z_g}$$

N-parallel grid connected converters modelling

Based on the Norton equivalent model of a single grid connected converter presented in Fig. 1(b), the equivalent impedance model of N-parallel converters can be obtained as shown in Fig. 3.

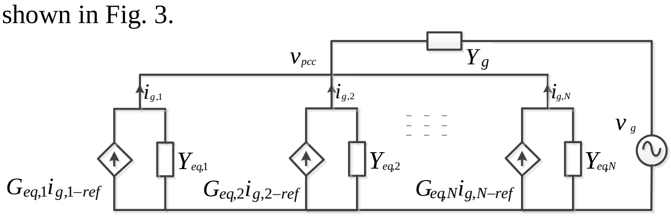

Fig. 3: Model of N-parallel grid connected converters.

Similar to a single grid connected model, the overall closed loop response of the i^{th} converter including the effect of grid impedance and other parallel converters can be obtained as:

$$i_{g,i} = R_i i_{\text{g,i-ref}} + P_{i,k}\, i_{\text{g,k-ref}} + S_{i,g}\, v_g \quad (6)$$

where:

$$R_i = \frac{i_{g,i}}{i_{\text{g,i-ref}}} = G_{eq,i}\left(1 - \frac{Y_{eq,i}}{Y_g + \sum_{k=1}^{N} Y_{eq,k}}\right),$$

$$P_{i,k} = \frac{i_{g,i}}{i_{\text{g,k-ref}}} = -\frac{Y_{eq,i} G_{eq,k}}{Y_g + \sum_{k=1}^{N} Y_{eq,k}}, k \in (1, N), k \neq i$$

$$S_{i,g} = \frac{i_{g,i}}{v_g} = -\frac{Y_{eq,i}\, Y_g}{Y_g + \sum_{k=1}^{N} Y_{eq,k}}$$

It can be seen that three different resonance terms are found in (6). R_i is the internal resonance and it represents the resonance introduced by a grid current reference change for the i^{th} converter. $P_{i,k}$ is the parallel resonance and it represents the resonance introduced to the grid current of the i^{th} converter due to grid current reference change of the k^{th} parallel converter. Finally, $S_{i,g}$ is the series resonance introduced from a grid voltage change to the injected grid current from the i^{th} converter. When a similar analysis is applied for each converter, the grid side current behaviour for all the converters can be derived in general matrix form as:

$$\begin{pmatrix} i_{g,1} \\ i_{g,2} \\ \vdots \\ i_{gN} \end{pmatrix} = \begin{pmatrix} R_1 & P_{1,2} & \cdots & P_{1,N} \\ P_{2,1} & R_2 & \cdots & P_{2,N} \\ \vdots & \vdots & \ddots & \vdots \\ P_{N,1} & P_{N,2} & \cdots & R_N \end{pmatrix} \begin{pmatrix} i_{\text{g,1-ref}} \\ i_{\text{g,2-ref}} \\ \vdots \\ i_{\text{g,N-ref}} \end{pmatrix} + \begin{pmatrix} S_{1,g} \\ S_{2,g} \\ \vdots \\ S_{N,g} \end{pmatrix} v_g \quad (7)$$

III. Design of Control Loops

This section presents the participatory design of the grid current controller and AD loops of each converter. Firstly, to avoid low frequency resonance and to ensure a high positive output admittance range, the grid current AD loop is designed to deal with the frequencies around the *LCL* resonance frequency based on the design guidelines recommend in[12, 15]. Therefore, the cut-off frequency of its HPF (ω_{adi}) is set at 0.3 of the sample frequency to achieve highest passivity range (i.e., positive Y_{eq}). Secondly, the capacitor voltage AD loop and current controller are designed simultaneously as the grid current AD loop is a part of the system plant. The cut off frequency of the capacitor voltage loop (ω_{adv}) is selected at 0.01 of the sample frequency to remove the fundamental component. The grid current gain k_{adi}, and capacitor voltage gain k_{adv} of the AD loops, and the grid current controller gain k_p are then optimized based on the root loci of the discrete z-domain model.

Discrete z-domain model

Fig. 4 illustrates the grid current control diagram for one converter in the discrete z-domain. A ZOH block and z^{-1} are included for modelling the digital PWM and computational delays [16]. The PR current controller $G_i(s)$ is discretised using the Tustin transformation prewarped at the fundamental frequency. The grid current active damper $G_{adi}(s)$ and the capacitor voltage active damper $G_{adv}(s)$ are discretised by applying the Tustin transformation while the plant transfer functions $G_{v_{inv}}^{i_g}(s)$ and $G_{v_{inv}}^{v_c}(s)$ are discretised by applying the ZOH transformation. The open loop $G'_{ol}(z)$ and closed loop $G'_{cl}(z)$ transfer functions of the grid current control with the proposed AD are:

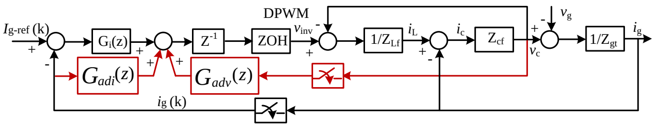

Fig. 4: z-domain grid connected converter control with AD.

$$G'_{ol}(z) = \frac{z^{-1}G_i(z)G_{v_{inv}}^{i_g}(z)}{1-z^{-1}G_{adi}(z)\,G_{v_{inv}}^{i_g}(z)-z^{-1}G_{adv}(z)\,G_{v_{inv}}^{v_c}(z)} \tag{8}$$

$$G'_{cl}(z) = \frac{z^{-1}G_i(z)G_{v_{inv}}^{i_g}(z)}{1+z^{-1}G_i(z)\,G_{v_{inv}}^{i_g}(z)-z^{-1}G_{adi}(z)\,G_{v_{inv}}^{i_g}(z)-z^{-1}G_{adv}(z)\,G_{v_{inv}}^{v_c}(z)} \tag{9}$$

where;

$$G_i(z) = k_p + k_r.\frac{\xi\sin(\omega_1 T_s)(z^2-1)}{[z^2-2z\cos(\omega_1 T_s)+1]+\xi\sin(\omega_1 T_s)(z^2-1)}$$

$$G_{v_{inv}}^{i_g}(z) = \frac{T_s}{(L_f+L_{gt})(z-1)} - \frac{(z-1)\sin(\omega'_{res}T_s)}{(L_f+L_{gt})\omega'_{res}[z^2-2z\cos(\omega'_{res}T_s)+1]}$$

$$G_{v_{inv}}^{v_c}(z) = \frac{[1-\cos(\omega'_{res}T_s)](z-1)}{L_f C_f {\omega'_{res}}^2[z^2-2z\cos(\omega'_{res}T_s)+1]}$$

$$G_{adi}(z) = \frac{2k_{adi}(z-1)}{z(\omega_{adi}T_s+2)+(\omega_{adi}T_s-2)}$$

$$G_{adv}(z) = \frac{2k_{adv}(z-1)}{z(\omega_{adv}T_s+2)+(\omega_{adv}T_s-2)}$$

$$\omega'_{res} = \sqrt{\frac{L_f+L_{gt}}{L_f L_{gt} C_f}}, \qquad L_{gt} = L_{fg} + L_g$$

Control system design procedures

For simplicity, the current controller is assumed to be a proportional gain only; the resonant term of the PR resonant controller is designed to achieve zero steady-state error at f_1 and its effect at higher frequency is small [17]. The participatory design procedures [18] are formulated as follows:

1- The grid current AD loop is designed to damp the resonance related to the *LCL*-filter (L_g=0). This is determined from the root locus at the point where the distance between the conjugate poles is minimum.

2- Based on the parameters from step 1, the capacitor voltage loop is designed at the critical resonance frequency ($f_{res} = f_s/6$), noting the grid current AD loop is now a part of the plant. The proportional current controller and the capacitor voltage AD loop gains are selected based again on the minimum distance between the conjugate poles.

The design for two different converters with parameters listed in Table I is carried out and used for the analysis and experimental tests. The root loci of the closed loop system using the parameters of 1st converter listed in Table I and the proposed design are shown in Fig. 5. The optimum root contours that represent the minimum distance between conjugate poles are marked by "x". From Fig. 5(a), the optimum value of k_{adi} is 10 and from Fig. 5(b) the optimum values of k_{adv} and k_p are 0.7 and 15.5 respectively. The same technique is used for the 2nd converter and summary of all gains are listed in Table II.

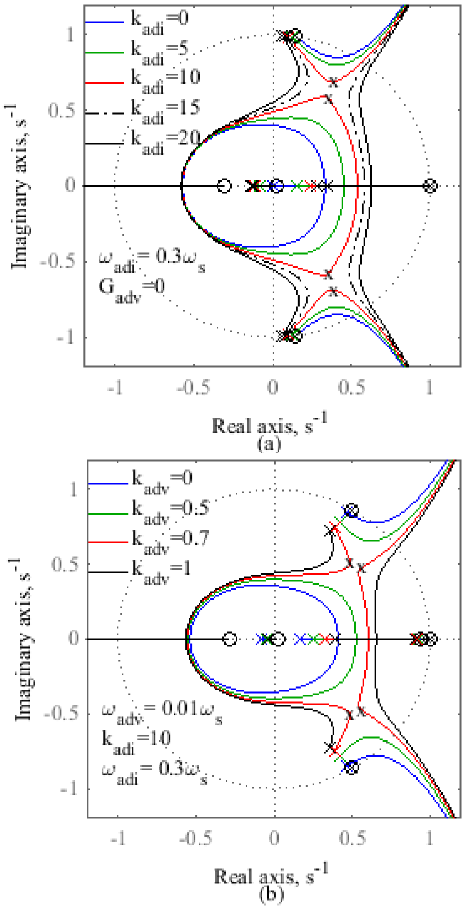

Fig.5. Root loci of closed loop system of converter 1.
(a) $G_{adi,1}$ design (step 1). (b) $k_{p,1}$ and $G_{adv,1}$ design (step 2).

Table I: System parameters

Parameter	Symbol	Value
Grid frequency	f_1	50 Hz
Converter-side filter inductor	$L_{f,1}$	5.7 mH
Grid-side filter inductor	$L_{fg,1}$	1 mH
Filter capacitor	$C_{f,1}$	5.8 µF
Converter-side filter inductor	$L_{f,2}$	4.6 mH
Grid-side filter inductor	$L_{fg,2}$	1mH
Filter capacitor	$C_{f,2}$	6 µF
Grid inductance	L_g	2.5 mH
Switching frequency	f_{sw}	10 kHz
Sampling frequency	f_s	10 kHz
Resonant gain	k_r	600
Damping factor	ξ	0.02

Table II: Controller parameters.

Parameter	Symbol	Value
Current controller P gain, 1st converter	$k_{p,1}$	15.5
Grid current AD gain, 1st converter	$K_{adi,1}$	10
Capacitor voltage AD gain, 1st converter	$K_{adv,1}$	0.7
Current controller P gain, 2nd converter	$k_{p,2}$	15
Grid current AD gain, 2nd converter	$K_{adi,2}$	10
Capacitor voltage AD gain, 2nd converter	$K_{adv,2}$	0.6

IV. Responses of Multiple Parallel Grid Connected Converters

In this section, the bode plots of different resonance terms presented in (6) for N-parallel grid connected converters are presented and analysed. It is assumed all converter have identical circuit and control parameters of converter one as given in Table I.

Investigation of resonance without damping

Fig. 6(a) shows the bode plots of the internal resonance transfer function R_i of the i^{th} converter with a different number of parallel grid connected converters. It can be seen that two resonance peak are appear. One of them has a fixed resonance frequency with constant amplitude and it is related to the *LCL*-filter resonance frequency. The frequency of the other peak moves to the low frequency region with a significant reduction of its amplitude as the number of parallel converters increases. It is worth mentioning that the worst case of this resonance effect will occur when only two converters are connected in parallel to the grid.

The bode plot of the parallel resonance transfer function $P_{i,k}$ from the k^{th} converter to the i^{th} converter for a different number of parallel grid connected converters is given in Fig. 6(b). It can be seen that two different peaks also appear. One has a fixed frequency with a significant decrease of its amplitude as the number of parallel converters increases. The other has a frequency which moves to the low frequency region with attenuated magnitude as more converters are connected in parallel. This can be explained from the equivalent impedance circuit shown in Fig. 3. When only two parallel converters are connected to the grid and one of them has a reference current step change, a part of the output current of this converter flows to the other converter and this case represents the worst case. As the number of parallel converters increases, the current flowing from this converter to the others will decrease as it will be shared by more parallel admittances. Therefore, the effect of one converter on the others will be reduced with increasing number of parallel grid connected converters.

The bode plot of the series resonance transfer function $S_{i,g}$ from the grid to the i^{th} converter for different numbers of parallel grid connected converters is depicted in Fig. 6(c). It can be seen that only one peak exists and its frequency moves toward the low frequency region with attenuated magnitude as more parallel converters are connected. With an increase in the number of parallel grid connected converters, the effect from the grid as well as from parallel converters to the i^{th} converter reduces.

Investigation of resonance with the proposed AD

The bode plot of the closed loop internal resonance transfer function with the proposed AD is shown in Fig. 7(a). The fixed resonance as well as the varying resonance peaks are well damped and their magnitudes are kept below 100 % (0 dB).

Fig. 7(b) shows the mitigation of parallel resonance from one converter to another for different numbers of parallel grid connected converters using the proposed AD technique. It can be seen that all resonance peaks are suppressed and kept at low amplitudes compared to their values without damping shown in Fig. 7.

Similarly, the series resonance from the grid to one converter for different number of parallel grid connected converters is well mitigated with the proposed AD technique as shown in Fig. 7(c). It is worth noting that beside series resonance reduction, low order harmonic rejection is also enhanced.

Generally, the proposed AD technique is effective in mitigating various resonance types and it can maintain stability for multiple *LCL*-filtered parallel grid connected converters.

V. Experimental Results

To validate the proposed AD method, two 3-phase power converters with *LCL*-filters shown in Fig. 8 has been built and connected to a Chroma 61511 programmable AC source using the system parameters of Table I. The designed control scheme was implemented using TMS320C6713 DSPs fitted with an Actel FPGA A3P400 based boards and Host Port Interface (HPI) daughter cards. Capacitor voltages and grid currents are measured and transformed to digital signals by 16 bit A/D converters and are transferred to DSP through the FPGA boards. Experimental results at different operating scenarios for single and two-parallel grid connected converters are presented and discussed.

Single grid connected converter with relatively low grid inductance

Fig. 9. Shows the experimental results for single grid connected converter when L_g = 1.5 mH and ω'_{res}= 0.16 ω_s which falls within the unstable region. It should be noted that the system will be totally unstable if the current gain is set at 15.5 (designed value) without the damping method. To verify this, the system is operated at a current gain of 11 and the results are shown in Fig. 9(a). The system is marginally stable meaning that it will be unstable if the current gain is increased. The system became totally stable and exhibit fast dynamic response with the proposed AD method as clearly shown in Fig. 9(b).

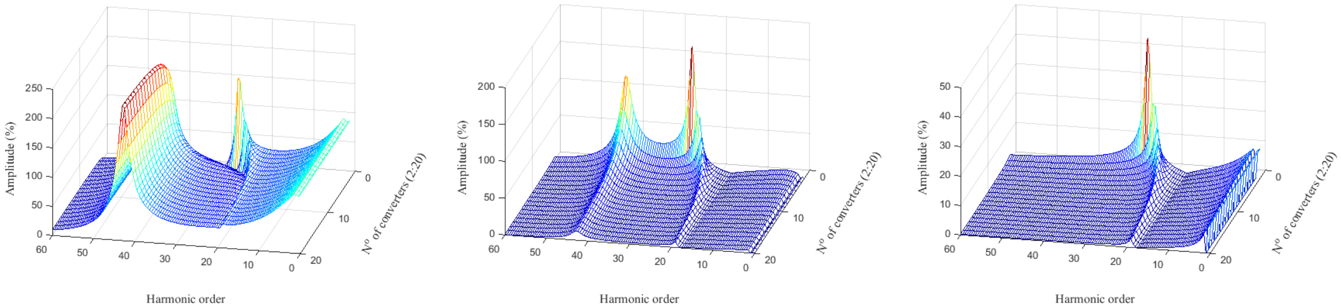

(a) (b) (c)

Fig. 6: Bode plots of resonance T.Fs without damping (a): Internal resonance. (b): Parallel resonance. (c): Series resonance.

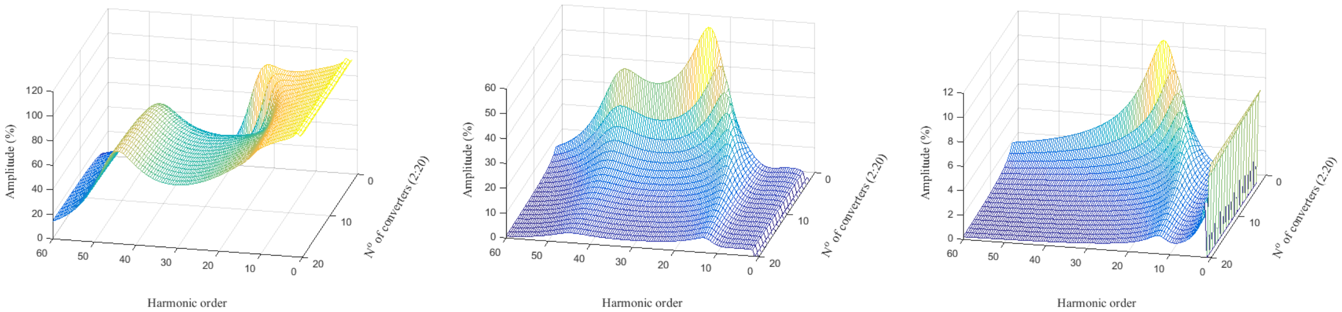

(a) (b) (c)

Fig. 7: Bode plots of resonance T.Fs with AD (a): Internal resonance. (b): Parallel resonance. (c): Series resonance.

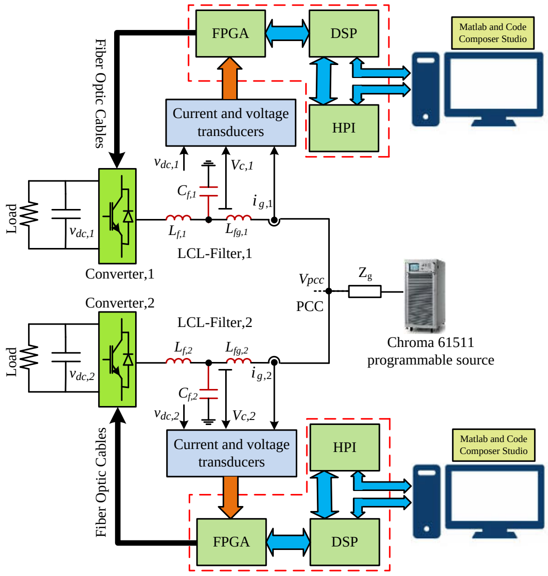

Fig. 8: Block diagram of experimental setup.

Single grid connected converter with relatively high grid inductance

Operation with a high grid impedance (L_g = 7.5 mH - i.e. weak grid) is also performed and the results are presented in Fig. 10. The system is marginally stable when operated without damping even if a lower current gain is used as shown in Fig. 10(a). However, the system becomes stable with the proposed AD method as can be seen from Fig. 10(b).

Investigation of internal and parallel resonance damping

In this test, the proposed AD loops of the two parallel converters are activated. The reference grid current of converter 1 is changed from 3 to 5A while the reference grid current of converter 2 is set at 5 A and results are shown in Fig. 11. It can be seen that system stability is maintained and the internal resonance is well damped (see $i_{g,1}$ in Fig. 11). As discussed before, the change of converter 1 reference current affects the injected grid current from converter 2 (parallel resonance). However, the transient in the grid current of converter 2 is well supressed ($i_{g,2}$ in Fig. 11) and stability of whole system is guaranteed thanks to the proposed AD.

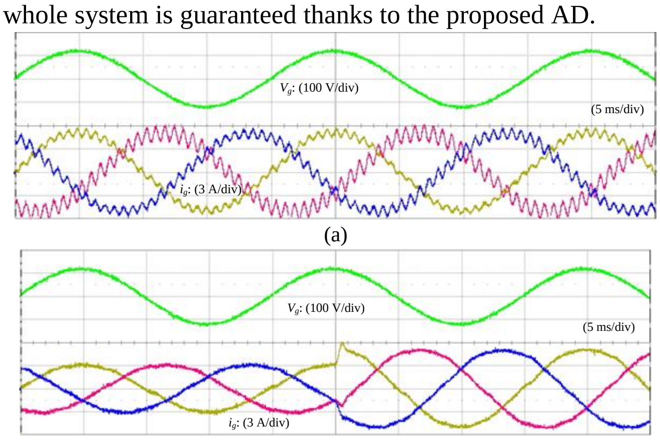

(a)
(b)

Fig. 9. Results for single grid connected converter with low L_g. (a) Without damping. (b) With the proposed AD.

Single grid connected converter with relatively high grid inductance

Operation with a high grid impedance (L_g = 7.5 mH - i.e. weak grid) is also performed and the results are presented in Fig. 10. The system is marginally stable when operated without damping even if a lower current gain is used as shown in Fig. 10(a). However, the system becomes stable with the proposed AD method as can be seen from Fig. 10(b).

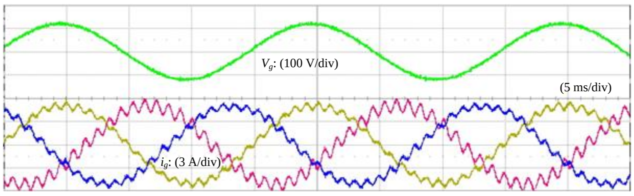

(a)

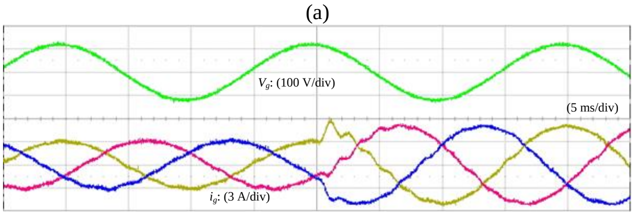

(b)

Fig. 10. Results for single grid connected converter with high L_g. (a) Without damping. (b) With the proposed AD.

Investigation of internal and parallel resonance damping

In this test, the proposed AD loops of the two parallel converters are activated. The reference grid current of converter 1 is changed from 3 to 5A while the reference grid current of converter 2 is set at 5 A and results are shown in Fig. 11. It can be seen that system stability is maintained and the internal resonance is well damped (see $i_{g,1}$ in Fig. 11). As discussed before, the change of converter 1 reference current affects the injected grid current from converter 2 (parallel resonance). However, the transient in the grid current of converter 2 is well supressed ($i_{g,2}$ in Fig. 11) and stability of whole system is guaranteed thanks to the proposed AD.

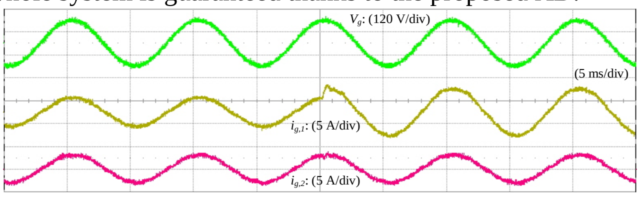

Fig. 11: Response to step change in the converter 1 grid current reference change.

Investigation of series resonance damping

In order to investigate the effect of the grid on the operation of parallel converters, a grid voltage sag of 10% is applied and results are given in Fig. 12. It is clearly seen that the associated dynamic responses of the injected grid current from converters 1 and 2 during the voltage sag are well damped.

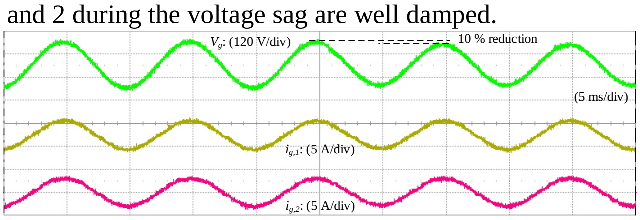

Fig. 12: Investigation of series resonance damping.

I. Conclusion

In this paper, a wide frequency range AD technique has been proposed to guarantee system stability and resonance damping for single and multiple parallel grid connected converters. Different resonance types created by multiple parallel grid connected converter have been investigated. The obtained time domain simulation and experimental results demonstrated the effectiveness of the proposed AD technique in terms of resonance damping and system stabilization.

References

[1] J. Xu, S. Xie, L. Huang, and L. Ji, "Design of LCL-filter considering the control impact for grid-connected inverter with one current feedback only," *IET Power Electronics,* vol. 10, pp. 1324-1332, 2017.

[2] M. Liserre, F. Blaabjerg, and S. Hansen, "Design and control of an LCL-filter-based three-phase active rectifier," *IEEE Transactions on Industry Applications,* vol. 41, pp. 1281-1291, 2005.

[3] D. Pan, X. Ruan, C. Bao, W. Li, and X. Wang, "Capacitor-Current-Feedback Active Damping With Reduced Computation Delay for Improving Robustness of LCL-Type Grid-Connected Inverter," *IEEE Transactions on Power Electronics,* vol. 29, pp. 3414-3427, 2014.

[4] H. Bai, X. Wang, and F. Blaabjerg, "Passivity Enhancement in Renewable Energy Source Based Power Plant With Paralleled Grid-Connected VSIs," *IEEE Transactions on Industry Applications,* vol. 53, pp. 3793-3802, 2017.

[5] Z. Bai, H. Ma, D. Xu, B. Wu, Y. Fang, and Y. Yao, "Resonance damping and harmonic suppression for grid-connected current-source converter," *IEEE Transactions on Industrial Electronics,* vol. 61, pp. 3146-3154, 2014.

[6] R. Peña-Alzola, M. Liserre, F. Blaabjerg, R. Sebastián, J. Dannehl, and F. W. Fuchs, "Analysis of the Passive Damping Losses in LCL-Filter-Based Grid Converters," *IEEE Transactions on Power Electronics,* vol. 28, pp. 2642-2646, 2013.

[7] W. Wu, Y. He, T. Tang, and F. Blaabjerg, "A New Design Method for the Passive Damped LCL and LLCL Filter-Based Single-Phase Grid-Tied Inverter," *IEEE Transactions on Industrial Electronics,* vol. 60, pp. 4339-4350, 2013.

[8] J. Dannehl, M. Liserre, and F. W. Fuchs, "Filter-Based Active Damping of Voltage Source Converters With LCL Filter," *IEEE Transactions on Industrial Electronics,* vol. 58, pp. 3623-3633, 2011.

[9] Y. Sato and T. Kataoka, "A current type PWM rectifier with active damping function," in *Industry Applications Conference, 1995. Thirtieth IAS Annual Meeting, IAS '95., Conference Record of the 1995 IEEE*, pp. 2333-2340 vol.3, 1995.

[10] M. Liserre, R. Teodorescu, and F. Blaabjerg, "Stability of photovoltaic and wind turbine grid-connected inverters for a large set of grid impedance values," *IEEE Transactions on Power Electronics,* vol. 21, pp. 263-272, 2006.

[11] X. Li, X. Wu, Y. Geng, X. Yuan, C. Xia, and X. Zhang, "Wide Damping Region for LCL-Type Grid-Connected Inverter With an Improved Capacitor-Current-Feedback Method," *IEEE Transactions on Power Electronics,* vol. 30, pp. 5247-5259, 2015.

[12] X. Wang, F. Blaabjerg, and P. C. Loh, "Grid-current-feedback active damping for LCL resonance in grid-connected voltage-source converters," *IEEE Transactions on Power Electronics,* vol. 31, pp. 213-223, 2016.

[13] J. Dannehl, F. W. Fuchs, S. Hansen, and P. B. Thogersen, "Investigation of active damping approaches for PI-based current control of grid-connected pulse width modulation converters with LCL filters," *IEEE Transactions on Industry Applications,* vol. 46, pp. 1509-1517, 2010.

[14] X. Wang, F. Blaabjerg, and P. C. Loh, "High-performance feedback-type active damping of LCL-filtered voltage source converters," in *2015 IEEE Energy Conversion Congress and Exposition (ECCE)*, pp. 2629-2636, 2015.

[15] J. Xu, S. Xie, and T. Tang, "Active damping-based control for grid-connected LCL-filtered inverter with injected grid current feedback only," *IEEE Transactions on Industrial Electronics,* vol. 61, pp. 4746-4758, 2014.

[16] D. M. V. d. Sype, K. D. Gusseme, A. R. V. d. Bossche, and J. A. Melkebeek, "Small-signal z-domain analysis of digitally controlled converters," in *2004 IEEE 35th Annual Power Electronics Specialists Conference (IEEE Cat. No.04CH37551)*, pp. 4299-4305 Vol.6, 2004.

[17] S. G. Parker, B. P. McGrath, and D. G. Holmes, "Regions of active damping control for LCL filters," *IEEE Transactions on Industry Applications,* vol. 50, pp. 424-432, 2014.

[18] A. Ghanem, M. Rashed, M. Sumner, M. A. Elsayes, and I. I. I. Mansy, "Hybrid active damping of LCL-filtered grid connected converter," in *2016 IEEE 2nd Annual Southern Power Electronics Conference (SPEC)*, pp. 1-6, 2016.